  Bull. Chem. Soc. Jpn., 53, 2241—2247 (1980)

Ion Pair Formation between Electro-generated 1,2-Naphtoquinone Anion Radicals and Alkali Metal Cations in Acetonitrile

Taitiro FUJINAGA, Satoshi OKAZAKI, and Tsutomu NAGAOKA*

Department of Chemistry, Faculty of Science, Kyoto University, Sakyo-ku, Kyoto 606

(Received December 24, 1979)

Ion association of 1,2-naphthosemiquinone with the alkali metal cations in acetonitrile has been comprehensively studied by the use of ESR, absorption spectroscopy, polarography and with MO calculation. A continuous flow electrolysis system with a glassy carbon column electrode has been developed for the rapid quantitative preparation of organic free radicals, whose ESR spectrum or absorption spectrum was observed *in situ*. The formation constants of the ion pair with K^+, Na^+, and Li^+ were estimated as $10^{3.2}$, $10^{4.5}$, and $10^{8.0}$, respectively. By the addition of alkali metal cations, the half-wave potentials shifted to more positive potential in the order of $K^+ < Na^+ < Li^+$. The proton hyperfine splitting constants in the ESR also varied in this order. This column electrolysis method is considered to be a powerful technique, particularly for the study of short lived free radicals, because the quantitative electrolysis is performed rapidly even in a solution of extremely diluted supporting electrolyte, such as 0.1 mM (mmol/dm^3).

In most of the studies of ion pair formation between organic free radicals and alkali metal cations by means of ESR and absorption spectroscopy, radical anions were usually obtained by chemical reactions with alkali metals using solvents, such as ether, having low dielectric constants.[1-3] Therefore, it is not particularly useful to carry out discussions of the comparisons of their characteristics with those obtained in polarography, in which dipolar aprotic solvents are generally used.

Fujinaga *et al.* have studied the electrolytic preparation of organic free radicals[4] and their electrochemical behavior in *N,N*-dimethylformamide by the use of ESR and polarography.[5] The effect of metal cations on the polarographic reduction of naphtoquinone in aprotic solvents have been investigated by Fujinaga *et al.*[6] and also recently, by Kalinowski *et al.*[7]

In the present paper, the authors employed a rapid flow electrolysis using a glassy carbon column electrode[8] in order to generate radical ions and studied the ion pair formation between 1,2-naphtoquinone radical anions (β-NPQ$^{-\cdot}$) and alkali metal cations of supporting electrolyte in acetonitrile by the comprehensive analysis of their ESR spectra and polarograms.

This column electrolysis method has the following advantages over the conventional constant potential electrolysis: 1) The objective depolarizers in the sample solution are completely electrolyzed immediately after flowing into the column; 2) The concentration of the electro-generated radical anion is determined by the simple monitoring of the electrolysis current instead of charge; 3) An ESR spectrum, or an absorption spectrum corresponding to the stepwise change of the electrode potentials can be observed *in situ*.

The formation constants of the ion pairs between β-NPQ$^{-\cdot}$ and alkali metal cations were inclined to increase with decreasing ionic radii of counterions, that is, $10^{3.2}$, $10^{4.5}$, and $10^{8.0}$ for K^+, Na^+, and Li^+, respectively. The proton hfs constants of their ESR spectra and half-wave potentials of their polarograms shifted significantly in the order of $K^+ < Na^+ < Li^+$. From these results, the complexes between β-NPQ anion and counter cations seem to be contact ion pairs.

Experimental

Reagents. Reagent grade β-NPQ from Wako Pure Chemicals, Ltd., Osaka was purified by the sublimation method. The concentration of β-NPQ used was 0.35 mM unless otherwise noted. Acetonitrile from the same supply was distilled over P_2O_5 after pretreated with calcium hydride. Propylene carbonate and *N,N*-dimethylformamid (DMF) were distilled under reduced pressure, after being dried with molecular sieves 4A. Tetraethylammonium perchlorate (TEAP) was prepared by the conventional method. All metal ions added were in their perchlorates. Other chemicals used were of analytical reagent grade.

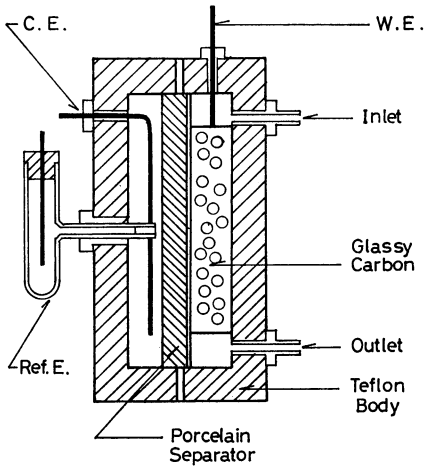

Fig. 1. Construction of flow-electrolysis cell.
(W. E.): Working electrode of carbon fibre, (C. E.): Pt wire counter electrode, and (Ref. E.): Ag/0.1 M $AgClO_4$ in acetonitrile (or DMF) reference electrode.

Apparatus. Figure 1 shows a vertical cross section of the column electrolysis cell made of a teflon body. Carbon fibres from Tokai Denkyoku Mfg. Co. Ltd., Nagoya were packed tightly and used as a working electrode. A platinum counter electrode and a reference electrode of Ag/0.1 M $AgClO_4$ in each solvent were used.

Figure 2 shows the block diagram of the flow cell system for ESR and absorption spectroscopic measurements. The parent quinone in the sample solution was electrolyzed immediately after flowing into the cell. Then electro-generated

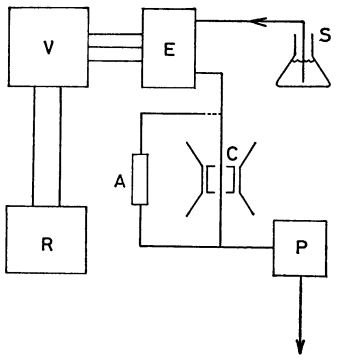

Fig. 2. Block diagram of flow system.
(E): Flow-electrolysis cell, (A): absorption cell, (C): ESR cavity, (S): sample reservoir, (V): potentiostat, (R): recorder, and (P): pump.

radical anion was sent into the cylindrical ESR cavity or the spectrophotometric flow-cell. The electrolysis current flowing through the cell was recorded by a National Pen Recorder Model VP 654-B. ESR spectra were measured with a JEOL JES-PE-3X, and the absorption spectra were measured with a Shimadzu UV 200 spectrophotometer. A PAR Model 174 Polarographic Analyzer was used for the measurements of polarograms. MO calculation was carried out by FACOM M-190 at the Data Processing Center of Kyoto University.

Results

Column Electrolysis and Absorption Spectroscopy. The fundamental examination of column electrolysis of β-NPQ were carried out by comparing the coulopotentiogram with its absorption spectrum. As a result, β-NPQ underwent two one-electron reductions in acetonitrile at glassy carbon electrode, and its electrolysis efficiency was 90—100% at the constant flow rate of 1.5 cm³/min.

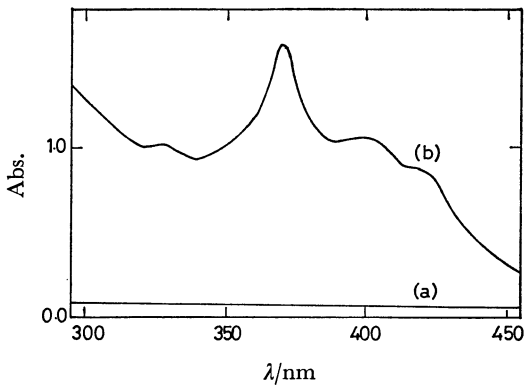

Fig. 3. UV absorption spectrum of β-NPQ$^{-\cdot}$ in acetonitrile with 0.1 M TEAP.
(a): Blank, and (b): 0.35 mM β-NPQ$^{-\cdot}$.

Figure 3 shows the absorption spectrum of electrogenerated β-NPQ$^{-\cdot}$ in acetonitrile with 0.1 M TEAP. The absorbance at 370 nm was proportional to the concentration of β-NPQ. By the addition of metal ion, the half-wave potentials of both waves shifted to more positive potentials owing to the ion pair formation effect. For the spectroscopic studies of ion pair formation of

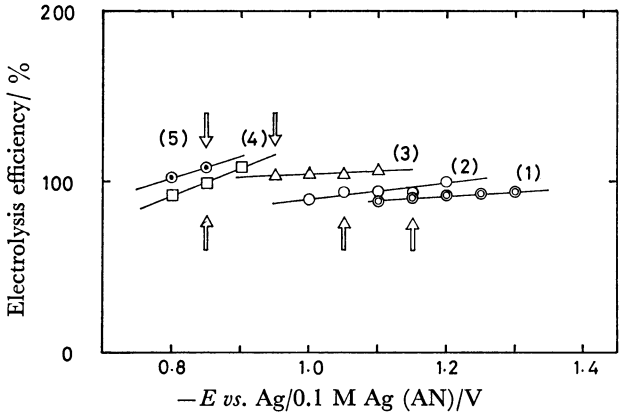

Fig. 4. Coulopotentiograms of β-NPQ$^{-\cdot}$ in acetonitrile with 0.1 M TEAP.
Concn of $LiClO_4$ in mM; (1): 0.0, (2): 0.06, (3): 0.15, (4): 0.3, and (5): 0.6.

monoanion radical, M^{+}·β-NPQ$^{-\cdot}$, the electrode potential was adjusted to maximize the absorption peak at 370 nm, which is inherent in the monoanion radical, β-NPQ$^{-\cdot}$. The same method was also adopted in ESR measurement.

Figure 4 illustrates the effect of lithium ions on the limiting current of the first wave, in which the arrow marks indicate the optimum potentials necessary to give the maximum intensity in the ESR spectra. As shown in the figure, the higher the lithium concentration, the narrower the available potential range to produce the monoanion radical alone became. With the addition of alkali metal, the absorption peak of β-NPQ$^{-\cdot}$ shifted to the shorter wave length, but within 10 nm.

ESR Spectroscopy. Figures 5-1 to 5-4 show the

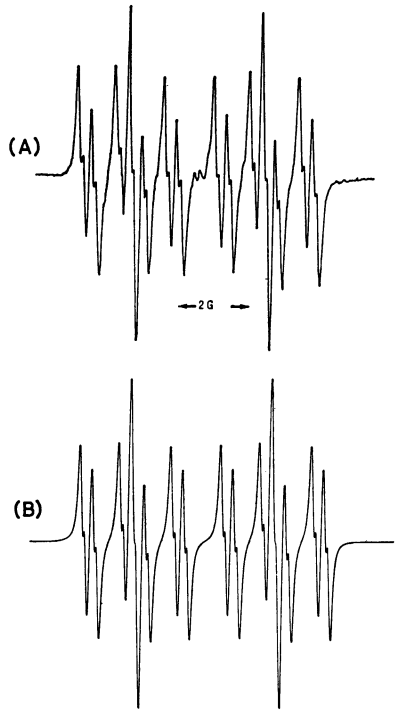

Fig. 5-1. Experimental (A) and simulated (B) ESR spectra of β-NPQ$^{-\cdot}$ in acetonitrile.
Concn of β-NPQ: 0.35 mM, 1 G=10^{-4} T.

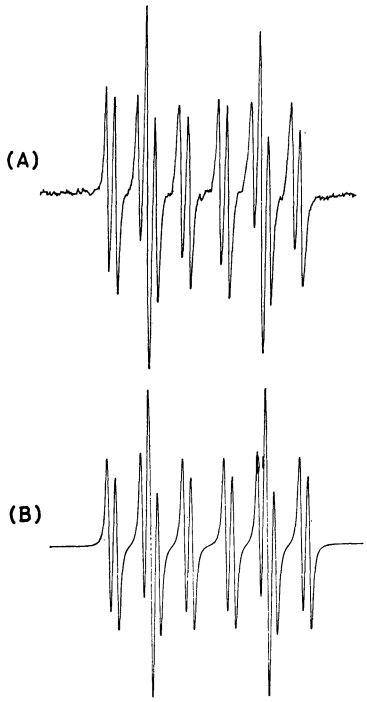

Fig. 5-2. Experimental (A) and simulated (B) ESR spectra of potassium ion pair in acetonitrile.
Concn of $KClO_4$: 3.0 mM.

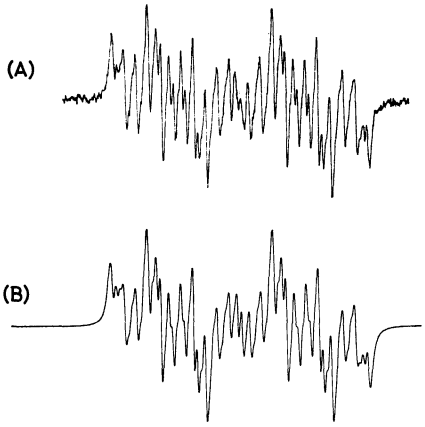

Fig. 5-3. Experimental (A) and simulated (B) ESR spectra of sodium ion pair in acetonitrile.
Concn of $NaClO_4$: 1.5 mM.

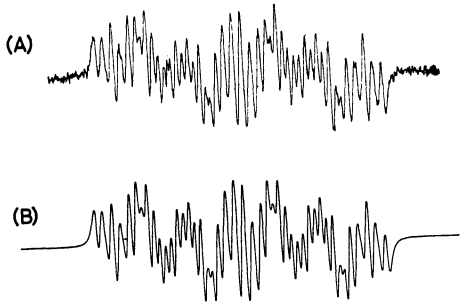

Fig. 5-4. Experimental (A) and simulated (B) ESR spectra of lithium ion pair in acetonitrile.
Concn of $LiClO_4$: 1.5 mM.

ESR spectra of β-$NPQ^{-\cdot}$ radical (5-1-A) and its potassium (5-2-A), sodium (5-3-A), and lithium (5-4-A) ion pairs together with their simulated spectra, from 5-1-B to 5-4-B, respectively. Good agreements were obtained between their observed spectra (A) and the corresponding simulated ones (B) within 20 mG (10^{-7} T). The fact that the spectrum of potassium ion pair (5-2-A) is similar to that of the free ion (5-1-A) suggests the weak association of β-NPQ radical anion with potassium cation. In the spectra of sodium and lithium ion pairs, however, each feature splits into four lines resulting from the coupling to ^{23}Na or ^{7}Li nuclei. The six ring-protons of the quinone are not equivalent, and these six proton hfs' are not all measurable. There were five protons with resolvable splittings for $Li^{+}\cdot\beta$-$NPQ^{-\cdot}$ and $Na^{+}\cdot\beta$-$NPQ^{-\cdot}$, whereas four for $K^{+}\cdot\beta$-$NPQ^{-\cdot}$.

When sodium or lithium perchlorate was added to the β-NPQ radical anion in acetonitrile, ESR signals due to both the free ion and its ion pair were observed simultaneously, as seen in Fig. 6-1-D. By the further addition of these cations, the intensity of the signal of the free anion was decreased, and only the spectrum of the ion pair was observed at the end. Figure 6-1-C shows the synthetic spectrum of β-$NPQ^{-\cdot}$ in the presence of 0.15 mM sodium ion, obtained by superimposing the simulated spectrum of the free ion (A) upon that of the sodium ion pair (B) on the assumption that the rate of the ion pair formation and dissociation of $Na^{+}\cdot\beta$-$NPQ^{-\cdot}$ is enough slow on the ESR time scale, *i.e.*, these two spectra can be simply superimposed upon each other.

In the case of the addition of potassium perchlorate, the ESR spectrum varied asymmetrically with respect

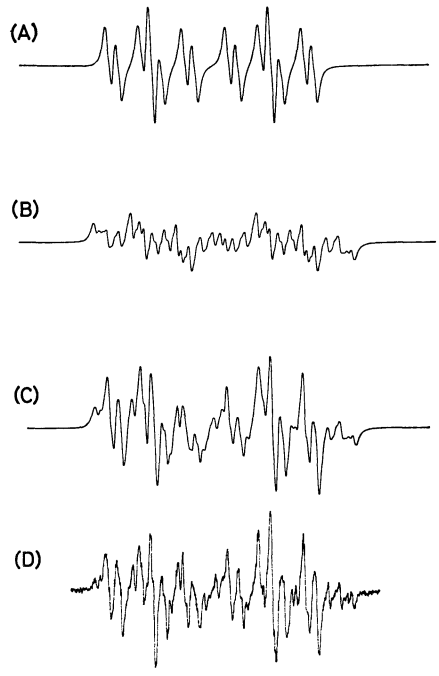

Fig. 6-1. Analysis of ESR spectrum of sodium ion pair. (A): Synthetic spectrum of free ion and (B): of sodium ion pair, (C): superimposed spectrum of (A) and (B), and (D): observed spectrum of sodium ion pair in the presence of 0.15 mM $NaClO_4$.

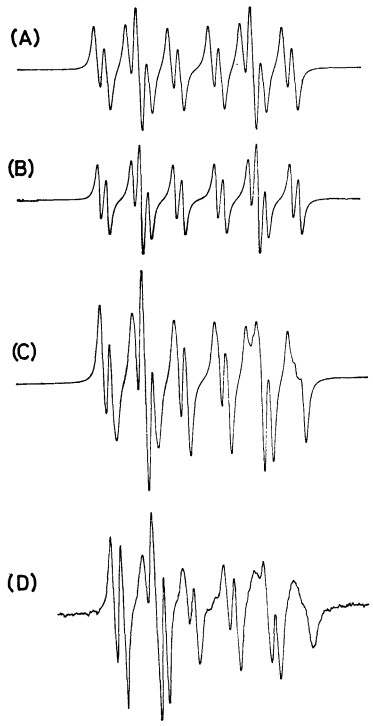

Fig. 6-2. Analysis of ESR spectrum of potassium ion pair. (A): Synthetic spectrum of free ion and (B): of potassium ion pair, (C): superimposed spectrum of (A) and (B), and (D): observed spectrum of potassium ion pair in the presence of 0.75 mM $KClO_4$.

to the line width. This asymmetry effect was most pronounced in the presence of about 0.75 mM potassium ions as seen in Fig. 6-2-D. This phenomenon suggests the coexistence of two radicals with slightly different coupling constants and *g*-values, *i.e.*, if the one having the smaller *g*-value possesses a larger coupling constant than the other, then the superposition of their ESR lines become loose at the region of high magnetic field. These two observed radicals were assigned to a free ion and an ion pair. Figure 6-2-C shows the synthetic spectrum of β-$NPQ^{-\cdot}$ in the presence of 0.75 mM potassium ion, obtained by the same method as in Fig. 6-1-C. Slight discordances were observed between the simulated (C) and observed (D) spectra owing to the line broadening at the region of high magnetic field. This fact suggests that the rate of the free ion–ion pair exchange kinetics of the potassium ion pair seems to be faster than those of the sodium and lithium ion pair, but still not to be so rapid as to give a time-averaged ESR spectrum.

MO Calculation. The proton hfs' in Table 1 were assigned by a HMO calculation adopting the McLachlan approximate configurational interaction. Table 2 summarizes the calculated results. The estimated value of the spin density of each carbon atom was very sensitive to given values of the coulomb integrals for two oxygen atoms (α_O). However, the spin density at position 6 defined in Fig. 7 was estimated still to be the largest even though the coulomb integral parameter (δ_O) was varied from 0.8 to 1.4. Therefore, the largest proton hfs constant in Table 1 is evidently assigned to the ring proton of position 6.

Table 1. Proton hyperfine spliting constants of $M^+\cdot\beta$-$NPQ^{-\cdot}$ in acetonitrile

Cation[a]	Proton hfsc (G)					Metal hfsc (G)
	a_6	a_5	a_7	a_9	a_{10}	a_M
TEA^+	4.05	1.49	1.12	0.34	0.11	0.00
K^+	4.16	1.49	1.20	0.29	≈0	≈0
Na^+	4.21	1.51	1.23	0.29	0.16	0.41
Li^+	4.43	1.57	1.40	0.24	0.35	0.59

a) Concentration of metal ions are 1.5 mM for lithium and sodium ion pairs and 3.0 mM for potassium ion pair.

Table 2. Calculated and observed hyperfine splitting constants

Position	HMO[a]		Exptl[c]
	Spin density	$\lvert a_H\rvert$[b] (G)	$\lvert a_H\rvert$ (G)
5	−0.0584	1.36	1.49
6	0.1739	4.05	4.05
7	0.0313	0.73	1.12
8	0.0023	0.05	—
9	0.0239	0.56	0.34
10	0.0095	0.22	0.11

a) $\alpha_O=\alpha_C+\delta_O\cdot\beta(\delta_1=0.8,\ \delta_4=1.1)$, $\beta_{C=O}=\gamma_{C=O}\cdot\beta$ ($\gamma_{C=O}=0.8$). b) $Q=23.3$, $\lambda=1.2$. c) With 0.1 M TEAP in acetonitrile.

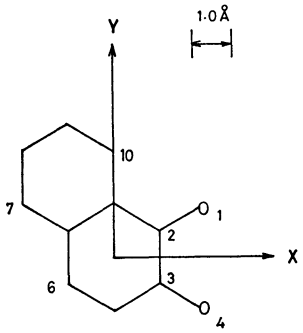

Fig. 7. Co-ordinate system for MO calculation of $M^+\cdot$ β-$NPQ^{-\cdot}$.
1 Å=10^{-10} m.

Variations of spin densities due to the ion pair formation can be discussed by means of the McClelland type MO calculation.[2,3,9] In this calculation, the effective Hamiltonian of the ion pair, H'_{eff} is defined by Eq. 1,

$$H'_{eff} = H_{eff} - \frac{Z\cdot e^2}{\varepsilon(r)\cdot r}, \qquad (1)$$

where, H_{eff} denotes the effective Hamiltonian in the absence of a cationic field, and $\varepsilon(r)$ is a screening factor introduced by Takeshita and Hirota[2] in order to explain the screening effect of solvent molecules on the anion. Figure 7 shows the co-ordinate system used in this calculation, in which a σ-type interaction was assumed and a positive point charge, $+e$ was approaching the anion along X-axis. Table 3 summarizes the results obtained by the use of this calculation, where $\varepsilon(r)$ was assumed to be constant, 10. The curves in Fig. 8 show the relationships between the calculated

Table 3. Variations of spin densities with the separation between cation and 1,2-naphtosemiquinone

Position	Å						
	∞	8.0	7.0	6.0	5.0	4.0	3.0
5	−0.0584	−0.0599	−0.0603	−0.0608	−0.0615	−0.0617	−0.0578
6	0.1739	0.1776	0.1789	0.1809	0.1844	0.1906	0.1995
7	0.0313	0.0337	0.0347	0.0362	0.0392	0.0455	0.0597
8	0.0023	0.0043	0.0049	0.0059	0.0077	0.0109	0.0162
9	0.0239	0.0231	0.0229	0.0226	0.0223	0.0221	0.0224
10	0.0095	0.0145	0.0162	0.0190	0.0240	0.0336	0.0521

$\varepsilon(r)=10.0$.

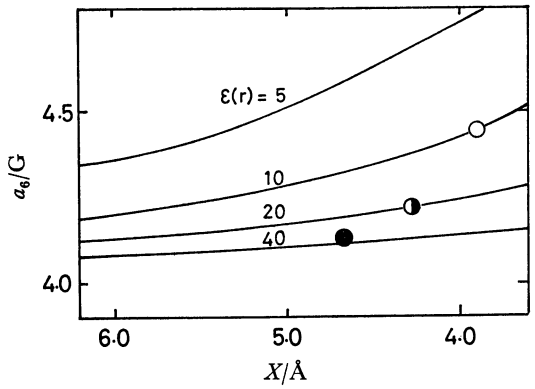

Fig. 8. Calculated and experimental proton hfs at position 6 as a function of interionic distance (X).
(○): Lithium, (◑): sodium and (●): potassium.

proton hfs at position 6 for each given value of $\varepsilon(r)$ and the interionic distance. In the figure, the experimental values are indicated by circles, the interionic distances of which were estimated on the assumption of a contact ion pair. From the results, it seems reasonable to consider $\varepsilon(r)$ for these ion pairs as an adjustable parameter being changed between 1 and the macroscopic dielectric constant of the solvent. This fact suggests the solvation tendency of acetonitrile toward these ion pairs. However, the quantitative discussions about $\varepsilon(r)$ are difficult owing to the rough approximation in the calculation.

Polarography. In acetonitrile, propylene carbonate, and DMF, β-NPQ undergoes two one-electron reductions corresponding to the formations of the stable monoanion and dianion. The polarographic characteristics for the reduction of the quinone are summarized in Table 4. The first wave was fairly reversible, but the second wave was less so in the solvents investigated, provided TEAP was used as the supporting electrolyte. When alkaline earth metals were used as the supporting electrolytes, both waves became less reversible than those with alkali metals. Both waves shifted to more positive potentials with increasing the concentration of the supporting electrolytes of metal salts, owing to their complex formation effects.

This potential shift was discussed according to Peover's method.[10] After the first one-electron reduction, the following complex formation equilibrium is assumed to be,

$$p\mathrm{M}^+ + \mathrm{Q}^{-\cdot} \overset{K}{\rightleftharpoons} \mathrm{M}_p\cdot\mathrm{Q}^{(p-1)+} \qquad (2)$$

Table 4. Polarographic data for the reduction of 1,2-naphtoquinone

Cation	$-E_{1/2}$ [b] V	I_d μA	Slope mV	ΔE_p [c] mV	I_c/I_a [d]
Acetonitrile					
Hex_4N^+	0.903	2.1	64	68	1.0
Pnt_4N^+	0.916	1.7	62	68	1.0
But_4N^+	0.903	1.9	61	70	1.0
Et_4N^+	0.908	1.9	60	68	1.0
Na^+	0.673	1.5	58	58	0.8
Li^+	0.492	1.7	54	82	0.5
Ba^{2+}	0.394	1.5	62	75	0.9
Mg^{2+}	0.083	2.0	77	85	1.3
Propylene carbonate					
Et_4N^+	1.323	0.62	64	68	1.0
Na^+	1.107	0.60	65	68	0.9
Li^+	0.985	0.60	83	75	0.6
N,N-Dimethylformamide					
Et_4N^+	0.955	1.60	63	73	1.1
K^+	0.886	1.65	65	68	1.3
Na^+	0.820	1.30	60	65	1.1
Li^+	0.758	1.30	60	68	1.0
Ba^{2+}	0.695	1.40	65	68	1.0
Sr^{2+}	0.650	1.68	62	88	≈1
Ca^{2+}	0.640	1.50	68	68	1.0
Mg^{2+}	0.576	1.20	76	190	1.0

a) Concn of β-NPQ: 0.35 mM in acetonitrile and propylene carbonate and 0.5 mM in DMF, concn of metal cation: 0.1 M. b) Potential was referred to Ag/0.1 M Ag^+ in each solvent. c) Potential difference between the anodic and cathodic peak of cyclic voltammmograms, sweep rate: 100 mV/s. d) Ratio of the cathodic (I_c) and anodic (I_a) peak current of cyclic voltammograms.

where, Q,$Q^{-\cdot}$ and $M_p\cdot Q^{(p-1)+}$ represent 1,2-naphthoquinone, its anion radical and ion pair, respectively, and p is a coordination number. The association constant K is given by Eq. 3,

$$K = \frac{[\mathrm{M}_p\cdot\mathrm{Q}^{(p-1)+}]}{[\mathrm{M}^+]^p\cdot[\mathrm{Q}^{-\cdot}]}. \qquad (3)$$

The shift of the half-wave potential, $\Delta E_{1/2}$ due to ion pair formation is given by Eq. 4,

$$\Delta E_{1/2} = -\frac{RT}{F}\ln\frac{[\mathrm{Q}^{-\cdot}]^\circ}{1/2[\mathrm{Q}]}, \qquad (4)$$

where $[Q^{-\cdot}]^\circ$ is the concentration of semiquinone at the electrode surface. When metal ions are in large excess,

$$\Delta E_{1/2} = \frac{RT}{F} \ln K + \frac{RT}{F} p \cdot \ln C_{M^+}. \quad (5)$$

A coordination number and an association constant are simply evaluated from the slope and intercept in the plot of the half-wave potential of β-NPQ *vs.* the logarithm of the concentration of metal ions, C_{M^+} as shown in Fig. 9.

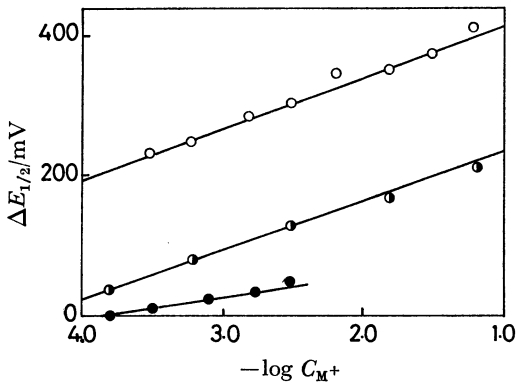

Fig. 9. Relationships between half-wave potentials of β-NPQ and concentrations of alkali metals.
Slopes in mV; 70 for Li^+ (○), 70 for Na^+ (◑) and 33 for K^+ (●).

Equation 5, however, cannot be used when a low soluble salt, *i.e.*, potassium perchlorate, is added in acetonitrile or when the coordination number varies at the low concentration of counterions. In these cases, the tentative association constant obtained from Eqs. 3 and 4, was converged by fitting p value so as to allow K to be nearly constant. This method could offer reliable association constants and coordination numbers even at a low concentration of counterions. These results are summarized in Table 5.

Table 5. Dependence of association constants of $M_p^+ \cdot \beta$-$NPQ^{-\cdot}$ on metal concentrations
0.35 mM β-NPQ in acetonitrile with 0.1 M TEAP.

Concentration (mM)	log K		
	Li^+	Na^+	K^+
0.150		4.62	
0.300	8.15		3.19
0.600	7.88	4.38	
0.750			3.18
1.50	7.99		3.17
3.00	7.97	4.49	3.18
15.0	7.99	4.52	
30.0	8.00		
60.0		4.66	
Coordination number	1.10	0.90	0.93

Discussion

The ion pair formation effects of supporting electrolyte cations with β-$NPQ^{-\cdot}$ were observed to be in the order of $TEAP^+ < K^+ < Na^+ < Li^+ < Ba^{2+} < Sr^{2+} < Ca^{2+} < Mg^{2+}$ as shown in Tables 1 and 4. The observed changes of proton hfs of ESR spectra in acetonitrile were somewhat larger than those in 1,2-dimethoxyethane (DME) reported by Warhurst *et al.*[1] This distinction between these two solvents is explained by the fact that the solvation of acetonitrile toward the ion pair is not more significant than DME as expected from their donor number; 14 for acetonitrile and 24 for DME. An unusual tendency of β-$NPQ^{-\cdot}$ for the coupling to metal nuclei also appeared in acetonitrile as well as in DME. This fact suggests the strong tendency of β-$NPQ^{-\cdot}$ toward ion pair formation, because it is not generally observed in these polar solvents. The variation of the coupling constants of ESR spectra are qualitatively well explained using a McClelland-type MO calculation. Table 3 shows a slight decrease in the spin density at position 9 but little increase at the other positions when a positive point charge approaches the β-NPQ anion along X-axis as illustrated in Fig. 7.

Polarography provides also much helpful information about the ion association equilibrium. Table 5 indicates that the association constants and the coordination numbers can be looked upon as being constant over the experimental concentration range of counterions. Therefore, it can be concluded that 1 : 1 type of ion pair is formed predominately between K^+ and β-$NPQ^{-\cdot}$, though 1 : 2 association may be expected from the slope of the plot in Fig. 9. The association constant for the potassium ion pair ought to be sufficiently accurate judging from a good accordance between the results obtained in polarography and ESR. As mentioned previously, the observed ESR spectrum is most asymmetric in the presence of 0.75 mM potassium ion, in which the signal intensities due to both the free ion and ion pair become almost equivalent. It is ascertained by calculation that the concentration ratio of free ion to ion pair is closed to unity in the presence of 0.75 mM potassium ion.

The relationships between the half-wave potentials and the effective ionic potentials $[\phi = Z/(r_c + S)]$[11,12] give straight lines with positive slopes as shown in Fig. 10. Though it is known that the ion pair with a contact structure gives a positive slope in this relation, a few comments will be needed here. Ion pairs may not always be in a form either solvent separated or contact, but may be intermediate between them. In this figure, the steeper slope for acetonitrile than DMF shows clearly that the association energy in acetonitrile is fairly large when compared to that in DMF, and moreover the solvation of the ion pair is more remarkable in DMF than in acetonitrile. As a result, the interionic distance between the cation and β-$NPQ^{-\cdot}$ anion may be larger in DMF than in acetonitrile. In this case, solvent molecules seem to act as pegs to separate the ion pair. In this study, the solvent effects on the half-wave potentials can be explained in terms of the difference in the solvation energies of these cations, because the solvation tendencies of DMF and acetonitrile to anions are almost equivalent.

The effect of the ionic size of the cation on the ion pair formation tendency will be discussed next. Simple MO calculations lead to the conclusion that the larger

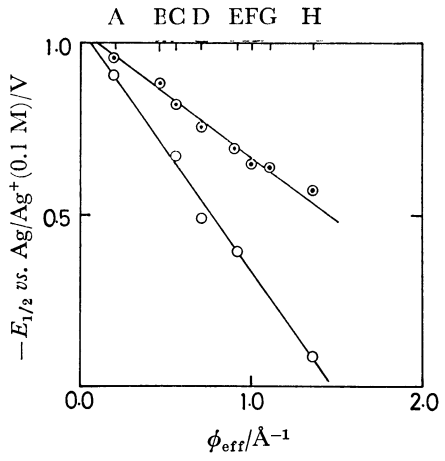

Fig. 10. Relationships between half-wave potentials of β-NPQ and effective ionic potentials of counterions.
(○): Acetonitrile, (⊙): DMF, correction parameter, $S=0.8$, (A): TEA^+, (B): K^+, (C): Na^+, (D): Li^+, (E): Ba^{2+}, (F): Sr^{2+}, (G): Ca^{2+}, (H): Mg^{2+}.

the radius of the counterion, the stronger the solvation of the ion pair become. That is to say, the structure of the potassium ion pair is looser than that of the lithium ion pair. As a result, the interionic distance of the potassium ion pair may be somewhat larger in fact than that given in Fig. 8. The structure of the potassium ion pair, however, is not a typical form of the solvent separated one, considering the contact structures of the ion pairs with sodium and lithium ions which have larger solvation energies than potassium.

The screening effects of the solvent molecules also seem to play an important role in this study. Toshima *et al.*[13] assume the $\varepsilon(r)$ value for the ion pair of nitrobenzene anion with alkali metal cations in DMF to be of the same order as the macroscopic dielectric constant of the solvent. In the ion pair considered here, however, $\varepsilon(r)$ should be regarded as an adjustable parameter.

It can be concluded that the smaller the ionic size of the counterion, the weaker the solvent separation of ion pairs becomes, *i.e.*, a so called contact ion pair is formed, and moreover the tendency of separation is dependent on the nature of the solvent used.

Recently, Chauhan *et al.*[14] reported on the weak association between nitromesitylene anion and tetraalkylammonium cation with the association constant of *ca.* 35. However, no complex formation effect of TEA^+ on the ESR spectrum of β-$NPQ^{-\cdot}$ was observed over the concentration range of TEAP from 10^{-4} M to 10^{-1} M.

It is also a great advantage of the column electrolysis that the electrolysis can be performed quantitatively even in the solution with a low concentration such as 10^{-4} M of the supporting electrolyte.

The present work was partially supported by a Grant-in-Aid for Scientific Research, No. 243010 from the Ministry of Education, Science and Culture.

References

1) E. Warhurst and A. M. Wilde, *Trans. Faraday Soc.*, **65**, 1413 (1969).
2) T. Takeshita and N. Hirota, *J. Am. Chem. Soc.*, **93**, 55 (1971).
3) "Ions and Ion Pairs in Organic Reactions," ed by M. Szwarc, John Weily and Sons, New York (1972), Vol. 1.
4) T. Fujinaga, Y. Deguchi, and K. Umemoto, *Bull. Chem. Soc. Jpn.*, **37**, 822 (1964).
5) T. Fujinaga, Y. Deguchi, and K. Umemoto, *Bull. Chem. Soc. Jpn.*, **46**, 2716 (1973).
6) T. Fujinaga, K. Izutsu, and T. Nomura, *J. Electroanal. Chem.*, **29**, 203 (1971).
7) J. S. Jaworski and M. K. Kalinowski, *J. Electroanal. Chem.*, **76**, 301 (1977).
8) T. Fujinaga, S. Okazaki, and T. Yamada, *Chem. Lett.*, **1972**, 836.
9) B. J. McClelland, *Trans. Faraday Soc.*, **57**, 1458 (1961).
10) M. E. Peover and J. D. Davies, *J. Electroanal. Chem.* **6**, 46 (1963).
11) M. K. Kalinowski, *Chem. Phys. Lett.*, **7**, 55 (1971).
12) T. M. Krygowski, M. Lipsztajn, and Z. Galus, *J. Electroanal. Chem.* **42**, 261 (1973).
13) S. Toshima, and K. Itaya, *Bull. Chem. Soc. Jpn.*, **49**, 957 (1976).
14) B. G. Chauhan, W. R. Fawcett, and A. Lasia, *J. Phys. Chem.*, **81**, 1476 (1977).